SANDIA REPORT
SAND2018-8563
Unlimited Release
Printed August 2018xx, 2018

Mechanical Characterization of Woven Composites at Different Temperatures

Helena Jin, Kevin Nelson, April Nissen, Brian Werner, Tim Briggs

Prepared by
Sandia National Laboratories
Albuquerque, New Mexico 87185 and Livermore, California 94550

Sandia National Laboratories is a multimission laboratory managed and operated by National Technology and Engineering Solutions of Sandia, LLC., a wholly owned subsidiary of Honeywell International, Inc., for the U.S. Department of Energy's National Nuclear Security Administration under contract DE-NA-0003525.

Issued by Sandia National Laboratories, operated for the United States Department of Energy by Sandia Corporation.

Available to DOE and DOE contractors from
U.S. Department of Energy
Office of Scientific and Technical Information
P.O. Box 62
Oak Ridge, TN 37831

Telephone: (865) 576-8401
Facsimile: (865) 576-5728
E-Mail: reports@osti.gov
Online ordering: http://www.osti.gov/scitech

Available to the public from
U.S. Department of Commerce
National Technical Information Service
5301 Shawnee Rd
Alexandria, VA 22312

Telephone: (800) 553-6847
Facsimile: (703) 605-6900
E-Mail: orders@ntis.gov
Online order: http://www.ntis.gov/search

SAND2018-8563x
Unlimited Release
Printed August 2018xx, 2018

Mechanical Characterization of Woven Composites at Different Temperatures

Helena Jin, Kevin Nelson, April Nissen, Brian Werner, Tim Briggs

Abstract

This work is to characterize the mechanical properties of the selected composites along both on- and off- fiber axes at the ambient loading condition (+25^{o}C), as well as at the cold (-54^{o}C), and high temperatures (+71^{o}C). A series of tensile experiments were conducted at different material orientations of 0^{o}, 22.5^{o,} 45^{o}, 67.5^{o}, 90^{o} to measure the ultimate strength and strain $\sigma_{f,}$ $\varepsilon_{f,}$ and material engineering constants, including Young's modulus $E,$ Poisson's ratio $\nu,$ The composite materials in this study were one carbon composite carbon (AS4C/UF3662) and one E-galss (E-glass/UF3662) composite. They both had the same resin of UF 3362, but with different fibers of carbon AS4C and E-glass. The mechanical loading in this study was limited to the quasi-static loading of 2 mm/min (1.3x10^(-3) in/s), which was equivalent to 5x10$^{(-4)}$ strain rate. These experimental data of the mechanical properties of composites at different loading directions and temperatures were summarized and compared. These experimental results provided database for design engineers to optimize structures through ply angle modifications and for analysts to better predict the component performance.

CONTENTS

FIGURES

TABLES

1. INTRODUCTION

Products made of composite materials are widely used in the state of the art technology. Sandia National Laboratories is also applying composites for weapon applications. In most cases, these components operate at nonambient temperature, which may cause thermal stresses or changes in mechanical properties. The degree to which the temperature affects the mechanical properties in each loading orientation, as well as the manner in which it does needs to be studied. In order to optimize the design of the structure that is made of composite materials, it is necessary to know the temperature dependence of the material properties in different loading orientations.

A carbon fiber reinforced polymer (CFRP) and a glass fiber reinforced polymer (GFRP) material consisting of an 8-harness satin weave prepreg configuration with an epoxy based resin (UF3362) were used for this investigation. Laminates were hand laid up from pre-cut ply kits made using a CNC controlled ply cutter to control geometry and fiber orientation. The materials were cured in the form of flat plates using a standard autoclave process at 350° F (ramped at 5° F/min and dwelled for 1 hour) and 45 psi of pressure. Prior to gelation, the autoclave pressure was turned on and the vacuum was vented to adequately eliminate void formation yet provide effective devolatilization. Standard practices of tooling plates, caul plates, release films, bleeder, and edge string bleeder were employed to adequately consolidate the laminate during cure. Edge embedded thermocouples were actively used to monitor and drive the cure of the laminates. Fiberglass end tabs were secondarily bonded to the cured laminates for gripping during tensile tests. Specimens were then wet diamond-saw cut from consolidated panels.

This work involved characterizing the temperature dependent composite material properties of one GFRP (E-glass/UF3662) and one CFRP (AS4C/UF3662), at three temperatures -54^{o}C, +25^{o}C, +71^{o}C. A series of tensile experiments were performed at these three temperatures along loading orientations of 0^{o}, 22.5^{o,} 45^{o}, 67.5^{o}, 90^{o}. The mechanical properties including E_{11}, E_{22}, G_{12}, v_{12}, v_{21}, $\sigma_{11}f$, $\sigma_{22}f$, $\varepsilon_{11}f$, and ε_{22f} were obtained from these experiments.

There were two batches of composite panels used in this study. First batch of composites were the panels in three orientations: 0°– warp direction, 90°-weft direction and 45°-direction. Three panels were fabricated for each of these loading orientations. Second batch of composites were the panels in the other two off-axis orientations: 22.5° and 67.5°. Two panels were fabricated for each orientation. These two batches of composites panels had the same fiber and resin material and both had four woven plies, but had some difference in the material processing. The first batch of composite panels were cured with a breather in contact with the panel so it sucked a lot of resin which caused higher volume fraction of fiber in these panels than those cured without a breather in the second batcher. This was also reflected in the difference of panel thickness between these two batches. The glass fiber composites from the first batch were about 1.2 mm thick and those from the second batch were about 1.4 mm thick. The carbon fiber composites from the first batch were about 1.4 mm thick and those from second batch were about 1.5 mm thick. The exact fiber volume fraction in these composite panels will be characterized in the future work. The fabricated composite panels used for the experiments are listed in Table 1 for the first batch and in Table 2 for the second batch, respectively.

Table 1: Laminate Sequence Numbering in First Batch

	Laminate Stack Sequence Numbering			
Resin	**Fiber**	**Stack Sequence**	**# Plies/Panel**	**Panel No**
UF-3362	Carbon-AS4C	[(0/90)2]s	4	**1**
UF-3362	Carbon-AS4C	[(0/90)2]s	4	**2**
UF-3362	Carbon-AS4C	[(0/90)2]s	4	**3**
UF-3362	Carbon-AS4C	[(90/0)2]s	4	**4**
UF-3362	Carbon-AS4C	[(90/0)2]s	4	**5**
UF-3362	Carbon-AS4C	[(90/0)2]s	4	**6**
UF-3362	Carbon-AS4C	[(45/-45)2]s	4	**7**
UF-3362	Carbon-AS4C	[(45/-45)2]s	4	**8**
UF-3362	Carbon-AS4C	[(45/-45)2]s	4	**9**
UF-3362	E-Glass	[(0/90)2]s	4	**10**
UF-3362	E-Glass	[(0/90)2]s	4	**11**
UF-3362	E-Glass	[(0/90)2]s	4	**12**
UF-3362	E-Glass	[(90/0)2]s	4	**13**
UF-3362	E-Glass	[(90/0)2]s	4	**14**
UF-3362	E-Glass	[(90/0)2]s	4	**15**
UF-3362	E-Glass	[(45/-45)2]s	4	**16**
UF-3362	E-Glass	[(45/-45)2]s	4	**17**
UF-3362	E-Glass	[(45/-45)2]s	4	**18**

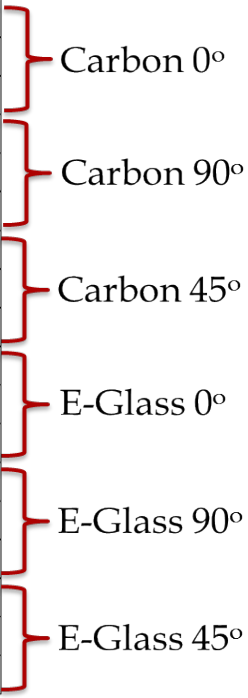

Table 2: Laminate Sequence Numbering in Second Batch

Laminate Stack Sequence Numbering in Second Batch				
Resin	**Fiber**	**Stack Sequence**	**# Plies**	**Panel No**
UF-3362	Carbon-AS4C	[(22.5/67.5)2]s	4	**CFRP 22.5 - 1**
UF-3362	Carbon-AS4C	[(22.5/67.5)2]s	4	**CFRP 22.5 - 2**
UF-3362	Carbon-AS4C	[(67.5/22.5)2]s	4	**CFRP 67.5 - 1**
UF-3362	Carbon-AS4C	[(67.5/22.5)2]s	4	**CFRP 67.5 - 2**
UF-3362	E-Glass	[(22.5/67.5)2]s	4	**GFRP 22.5 - 1**
UF-3362	E-Glass	[(22.5/67.5)2]s	4	**GFRP 22.5 - 1**
UF-3362	E-Glass	[(67.5/22.5)2]s	4	**GFRP 67.5 - 1**
UF-3362	E-Glass	[(67.5/22.5)2]s	4	**GFRP 67.5 - 1**

2. SPECIMEN PREPARATION

The composite panels with various fiber/matrix combinations were individually sanded and labeled. The end tabs of Garolite G10 were attached to both ends. The end tab strips were 50 mm wide by 3.5 mm thick. They were sanded on one side and adhered to the panel with Hysol 9309.3 NA adhesive using a jig to verify proper alignment during the adhesive cure. The tabbed composites panels were initially trimmed with a diamond-bladed wet saw to produce edges that were parallel to the specimen direction. They were machined into the desired panel sizes (8" Lx 1" W) and then were sliced into equal width of 25 mm. Figure 1 shows the representative carbon and glass fiber composite panels and the tensile specimens machined out of these panels.

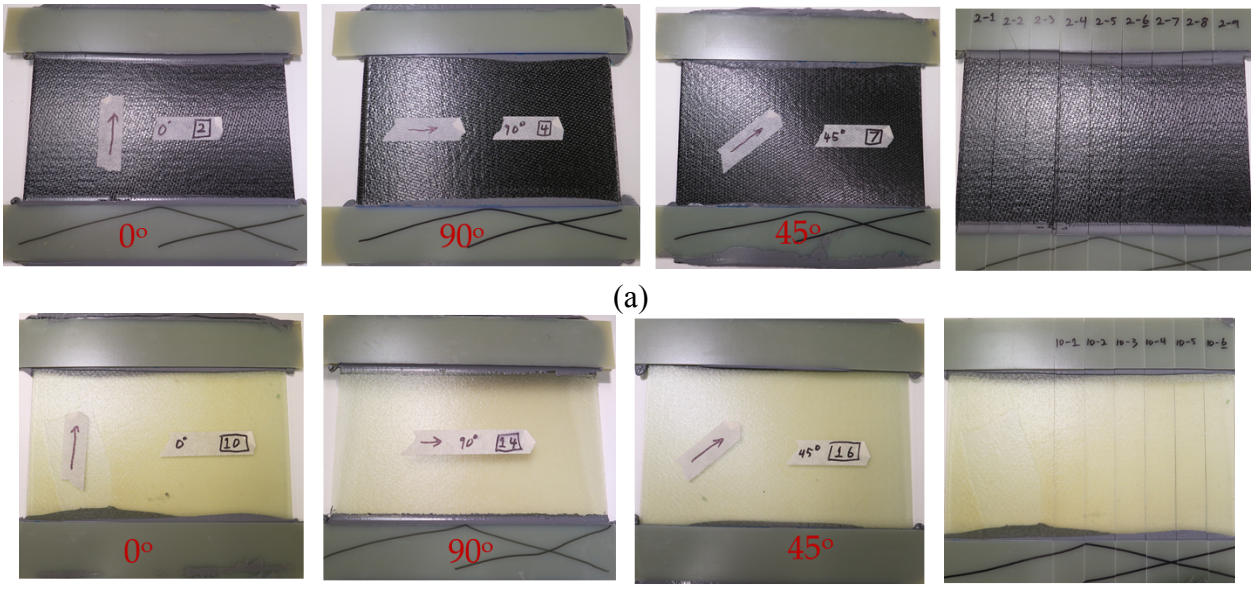

Figure 1: The tabbed composite panels at 0°, 45° and 90° and tensile specimens: (a) Carbon composite; (b) E-glass composite;

3. MECHANICAL TESTING

3.1. Experimental Setup

The mechanical characterization of the composite specimens at different temperatures was performed using Instron at the Structure Mechanics lab because it was able to incorporate a large temperature chamber. Instron also had the load capacity and displacement control needed for this set of experiments. Figure 2(a) shows the experimental setup for the mechanical testing at the non-ambient temperatures. The experiment was conducted inside a thermal chamber to maintain constant temperature during the test. Liquid nitrogen was used to cool the chamber down to -54^{o}C and hold constantly at this temperature. Heating lamp was applied to heat up the chamber to +71^{o}C for experiments at hot temperature. The chamber temperature was well maintained at constant temperature during each experiment. The specimens were clamped at the end tab from both ends. The mechanical loading was under displacement control with loading rate of 2 mm/ min, the equivalent strain rate was about $5x10^{(-4)}$/s. The global load and displacement of the specimen were recorded by Instron.

As shown in Figure 2(b), in the initial experimental setup, multiple techniques were applied to measure the displacement and strain. Laser extensometer, axial mechanical extensometer and strain gage were set up measure the axial strain. Strain gage and transverse extensometer were set up to measure the transverse strain. Each of these strain measurement techniques has its own strength and weakness. Strain gage had the best resolution of $10^{(-5)}$ but it can only measure strains up to a few percent. Therefore, it was a great technique to measure small strains. Mechanical and laser extensometers have a little less resolution, but with large strain range. They can be applied to measure large strains of 10% or more. In the first few experiments, the strains were measured using these different techniques. They were compared and showed nice consistency between different techniques. The mechanical extensometers had enough resolution to measure the small strains in the composite. Attaching the strain gage was more time consuming than setting up the extensometers. Therefore, after the initial few experiments for verifying these strain measurement techniques, laser and mechanical extensometers were applied to measure the strains in the composite for the rest of experiments.

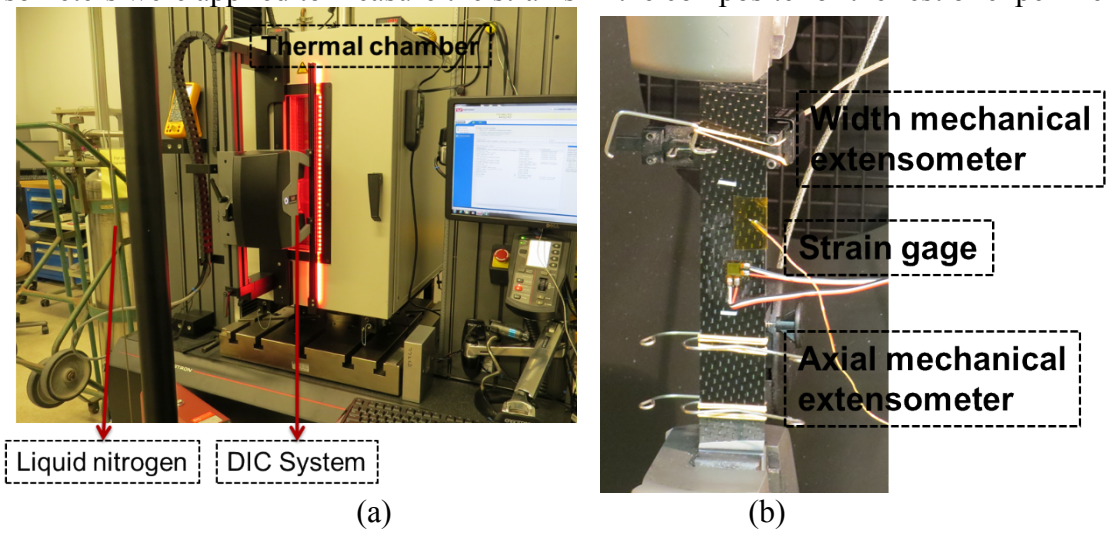

Figure 2. Experimental setup for non-ambient temperatures, (a) Thermal chamber; (b) Strain measurement on the specimen

3.2. Experimental Results from Mechanical Testing at Different Temperatures and Loading Directions

For each loading orientation and temperature, at least three specimens from the same composite material were tested to generate average value. The stresses were calculated from the global load. The strains were measured from the above strain measurement techniques. The stress versus strain curve was obtained from each specimen. The mechanical parameters including ultimate axial stress and axial strain, ultimate transverse strain σ_{11f}, σ_{22f}, ε_{11f}, ε_{22f} can be directly obtained from these curves. Then Young's modulus and Poisson ratio E_{11}, E_{22}, G_{12}, υ_{12}, υ_{21} were calculated by fitting the linear portion of stress versus strain and axial versus transverse strain curves respectively.

There were a large number of experiments performed in order to characterize the mechanical properties of the composites at different temperatures and loading orientations. It will be overwhelming to display all the details of the experimental data. Therefore, only two sets of experimental data were shown in detail to demonstrate how the mechanical properties were calculated and how they vary at different loading directions and temperatures. The first set of experiment data was from the carbon fiber composite loaded at cold temperature of -54°C, but at different loading directions of 0°, 22.5°, 45°, 67.5°, 90° to demonstrate the mechanical properties at different loading directions. The second set of experimental data was from the glass fiber composite loaded along 0°, but at different temperatures of -54°C, +25°C, +71°C to demonstrate the temperature effect. For the rest of tests, the experimental data from each specimen is not shown in detail in this report, but the results are summarized and compared in Tables and Figures.

Figure 3(a) shows the axial stress versus strain curves for the carbon fiber composite specimens loaded at -54°C along 0° direction. These stress versus strain curves from each specimen were linear and consistent with each other. The ultimate stresses (σ_{11f}) and strains (ε_{11f}) were obtained from the stress versus strain curves directly. Figure 3(b) shows the axial ~ transverse strain curves for the carbon fiber composite specimens loaded at -54°C along 0° direction. There was a relatively larger discrepancy in the axial ~ transverse strain curves. Partially it was due to the uncertainty of the transverse strain measurement. It can also be clearly seen that the curves were deviating away from the initial linear lines. These were caused by the error in transverse strain measurement. The deformation of the specimen caused the motion of the transverse extensometer which led to the error in strain measurement. However, only the initial linear portion of the axial ~ transverse strain curves were needed to calculate the Poisson's ratio. Young's modulus and Poisson ratios were calculated by fitting the linear portion of stress ~ strain and axial ~ transverse strain curves respectively. The mechanical values of carbon fiber composite specimens loaded at -54°C along 0° direction that were obtained from the linear portion of the curves in Figure 3. These mechanical properties are listed in Table 3, with values from each specimen, as well as the average value and the standard deviation.

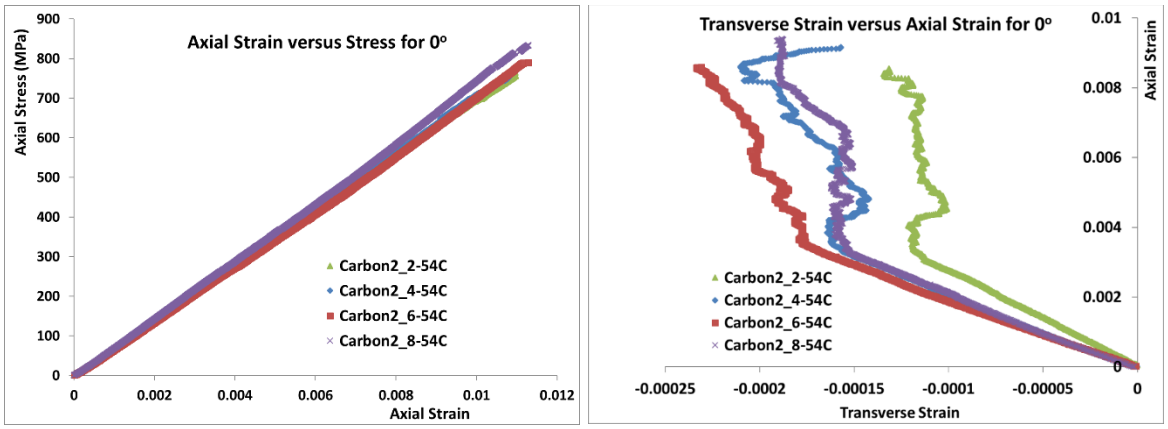

(a) (b)

Figure 3. (a) Axial strain versus stress, (b)Transverse strain versus axial strain for carbon composite (UF-3362/Carbon-AS4C) specimens loaded along 0° at -54°C

Table 3. The measured mechanical parameters values for carbon composite (UF-3362/Carbon-AS4C) specimens loaded along 0° at -54°C.

		(-54C) Plate #2 - 0^0			
Sample	**Ultimate Axial Strain**	**Ultimate Trans strain**	**Ultimate Stress (Mpa)**	**Youngs modulus (Gpa)**	**Poisson Ratio**
C2-8	0.01125	0.00023	831	72	0.045
C2-2	0.01100	0.00016	756	70	0.035
C2-4	0.01106	0.00020	770	70	0.046
C2-6	0.01112	0.00028	790	68	0.050
Average	0.01111	0.00022	787	70	0.0439
Standard deviation	0.00011	0.00005	33	2	0.0065

Similarly, four specimens from carbon fiber composite were tested at -54°C along 90° direction. Figure 4(a) shows the axial stress versus strain curves for these specimens. These curves were also linear and consistent with each other. The ultimate stresses (σ_{22f}) and strains (ε_{22f}) along 90° were obtained from the stress versus strain curves directly. Figure 4(b) shows the axial ~ transverse strain curves for these specimens. They also have large standard deviation as those loaded along 90° direction in Figure 3(b). The mechanical properties of carbon fiber composites that were tested at -54°C along 90° direction were calculated from the linear portion of the curves and were summarized in Table 4, with values of each specimen, as well as the average and standard deviation.

Table 4. The measured mechanical parameters values for carbon composite (UF-3362/Carbon-AS4C) specimens loaded along 90° at -54°C.

		(-54C) Plate #4 - 90^0			
Sample	Ultimate Axial Strain	Ultimate Trans strain	Ultimate Stress(Mpa)	Youngs modulus(Gpa)	Poisson Ratio
C4-5	0.01213	0.00052	856	71	0.066
C4-6	0.01248	0.00028	879	65	0.041
C4-7	0.01220	0.00056	850	67	0.068
C4-8	0.01164	0.00023	857	66	0.036
Average	0.01211	0.00040	861	67	0.0527
Standard deviation	0.00035	0.00017	13	2	0.0164

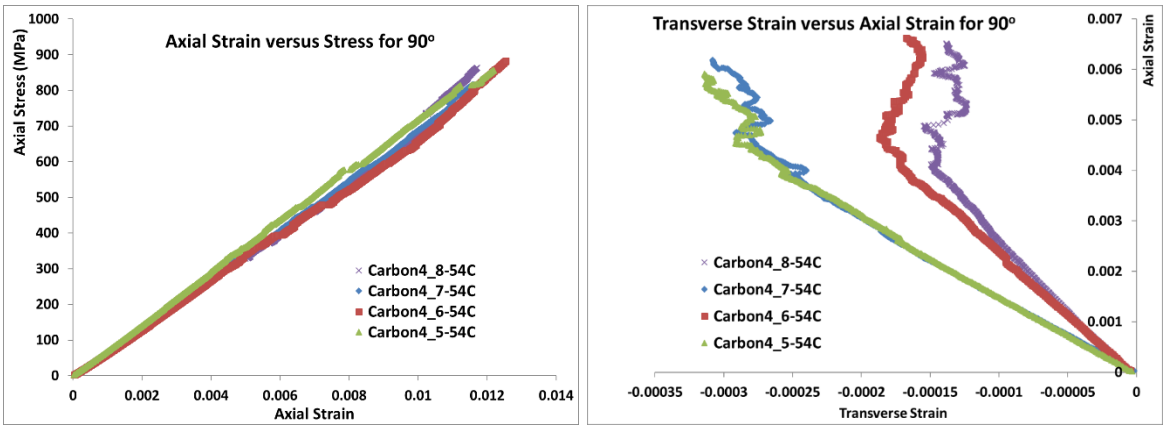

Figure 4. (a) Axial strain versus stress, (b)Transverse strain versus axial strain for carbon composite (UF-3362/Carbon-AS4C) specimens loaded along 90° at -54°C.

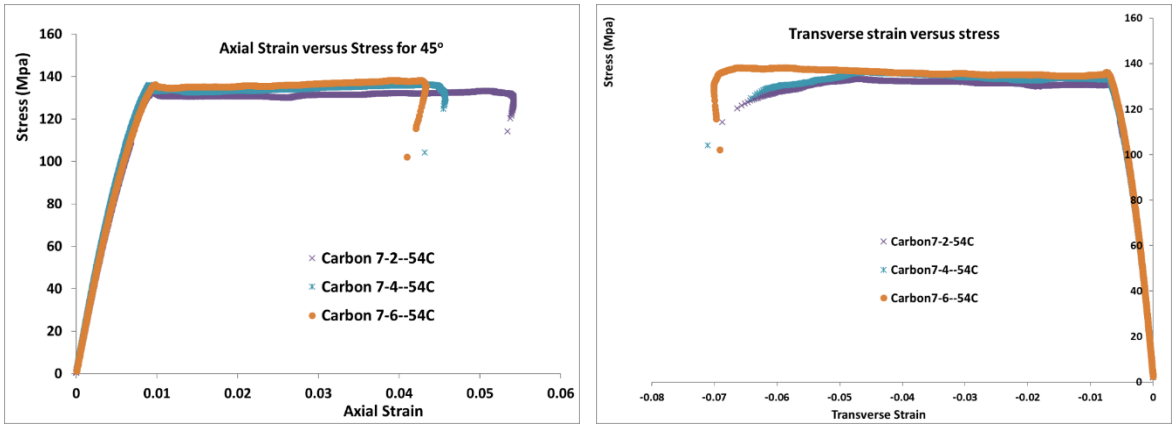

Figure 5. (a) Axial strain versus stress, (b)Transverse strain versus axial stress for carbon composite (UF-3362/Carbon-AS4C) specimens loaded along 45° at -54°C.

Table 5. The measured mechanical parameters values for carbon composite (UF-3362/Carbon-AS4C) specimens loaded along 45° at -54°C.

		(-54C) Plate #7 - 45^0			
Sample	Ultimate Axial Strain	Ultimate Trans strain	Ultimate Stress(Mpa)	Youngs modulus(Gpa)	Poisson Ratio
C7-2	0.05400	0.00709	133	17	0.696
C7-4	0.04400	0.00733	135	18	0.761
C7-6	0.04000	0.00773	136	18	0.703
Average	0.04600	0.00738	135	18	0.720
Std dev	0.00721	0.00032	2	1	0.0360

Similar to the above tests, three specimens from carbon fiber composite were tested at (-54°C) along 45° direction. Figure 5(a) shows the axial stress versus strain curves for these specimens. These curves were first linear and then flat. They were consistent with each other. The ultimate stresses (σ_{45f}) and strains (ε_{45f}) along 45° were obtained from the stress versus strain curves directly. The Young's moduli were calculated from the linear portion of the stress versus strain curves. Figure 5(b) shows the transverse strain versus axial stress curves for these specimens. The transverse moduli were calculated from the initial linear portion of the curves. The mechanical properties of carbon fiber composites that were tested at -54°C along 45° direction are summarized in Table 5, with values of each specimen, as well as the average value and standard deviation.

Specimens were also fabricated from the carbon fiber composite plate with 22.5° and 67.5° fiber orientations to characterize the mechanical properties in these two directions. Figure 6 and Figure 7 displayed the stress versus axial strain and transverse strain curves for the specimens along 22.5° and 67.5° respectively. The curves from these specimens were consistent with each other. The ultimate stress (σ_f) and strain (ε_f) were obtained from the stress versus strain curve directly. The Young's, transverse moduli and Poisson's ratio were calculated from the linear portion of the stress versus strain curve. The mechanical properties of carbon fiber composites that were tested at -54°C along 22.5° and 67.5° were summarized in Table 6 and 7 respectively, with value from each specimen, as well as the average and standard deviation.

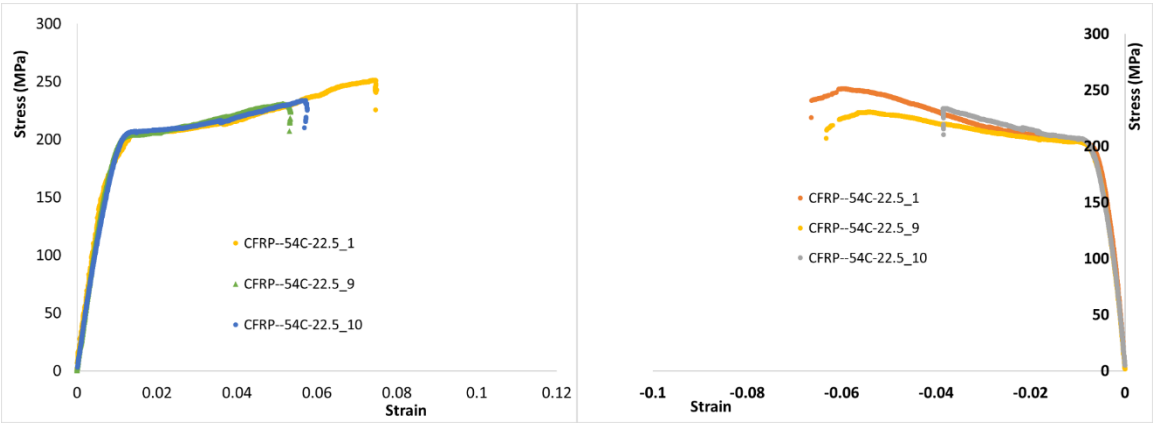

Figure 6. (a) Axial strain versus stress, (b)Transverse strain versus axial stress for carbon composite (UF-3362/Carbon-AS4C) specimens loaded along 22.5° at -54°C.

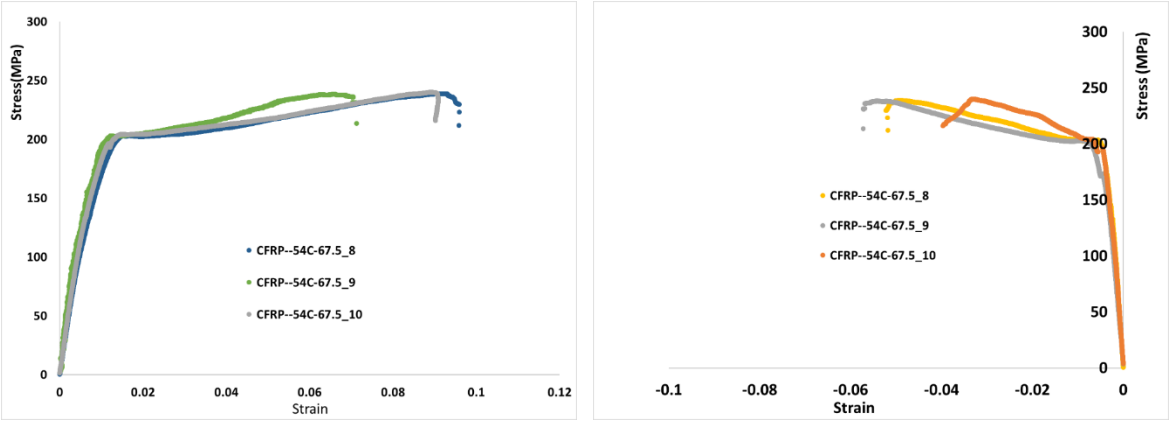

Figure 7. (a) Axial strain versus stress, (b)Transverse strain versus axial stress for carbon composite (UF-3362/Carbon-AS4C) specimens loaded along 67.5° at -54°C.

Table 6. The measured mechanical parameters values for carbon composite (UF-3362/Carbon-AS4C) specimens loaded along 22.5° at -54°C.

		(-54C) Plate 22.5^0			
Sample	Ultimate Axial Strain	Ultimate Trans strain	Ultimate Stress(Mpa)	Youngs modulus (Gpa)	Poisson Ratio
CFRP--54C-22.5_1	0.0670	0.0600	250	24	0.615
CFRP--54C-22.5_9	0.0530	0.0600	228	22	0.645
CFRP--54C-22.5_10	0.0570	0.0350	233	20	0.606
Average	0.0590	0.0517	237	22	0.6221
Std dev	0.0072	0.0144	12	2	0.0203

Table 7. The measured mechanical parameters values for carbon composite (UF-3362/Carbon-AS4C) specimens loaded along 67.5° at -54°C.

Sample	Ultimate Axial Strain	Ultimate Trans strain	Ultimate Stress (Mpa)	Youngs modulus (Gpa)	Poisson Ratio
CFRP--54C-67.5_8	0.09300	0.05500	237	17.8	0.339
CFRP--54C-67.5_9	0.06700	0.05670	235	21.5	0.497
CFRP--54C-67.5_10	0.08000		239	20.9	0.430
Average	0.08000	0.05585	237	20.1	0.4218
Std deviation	0.01300	0.00120	2	2.0	0.0791

The above Figures 3-7 showed the stress versus strain curves for the Carbon composites that were loaded along different directions at -54°C. The mechanical parameters measured or calculated from these curves were listed in Tables 3-7. In the same manner, carbon composite specimens were also tested at 25°C and 71°C along the loading directions of 0°, 22.5°, 45°, 67.5°, 90°. The stress versus strain curve for each specimen was not shown in detail here. But the mechanical parameter values are summarized in next session.

Similarly, glass fiber composite specimens were also characterized along different loading directions of 0°, 22.5°, 45°, 67.5°, 90° at three temperatures of -54°C, 25°C and 71°C. The axial stress versus strain and the axial strain versus transverse strain curves for glass fiber composite specimens loaded along 0° at three temperatures of -54°C, 25°C and 71°C are shown in Figures 8-10. It can be clearly seen that stress~strain curves are bilinear. The modulus and Poision's ratio were calculated from the initial linear portion of the curves and the measured mechanical property values are listed in Tables 8-10 for each temperature respectively.

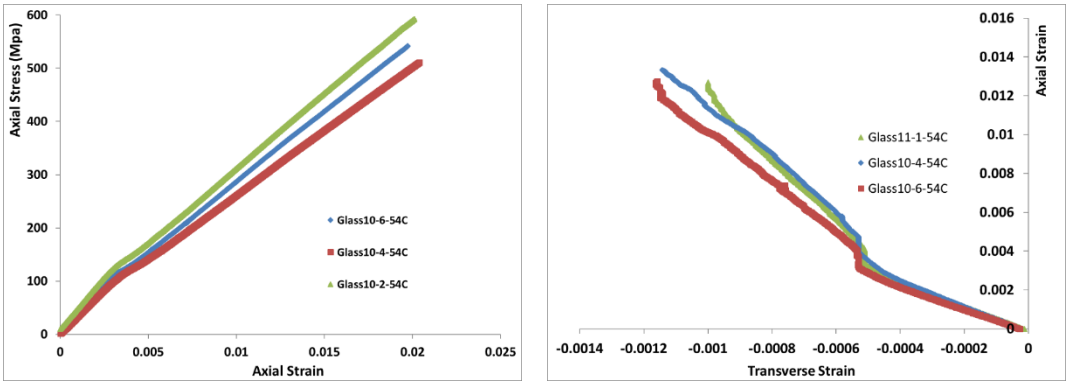

Figure 8. (a) Axial strain versus stress, (b) axial versus transverse strain for glass fiber composite (UF-3362/E-glass) specimens loaded along 0° at -54°C.

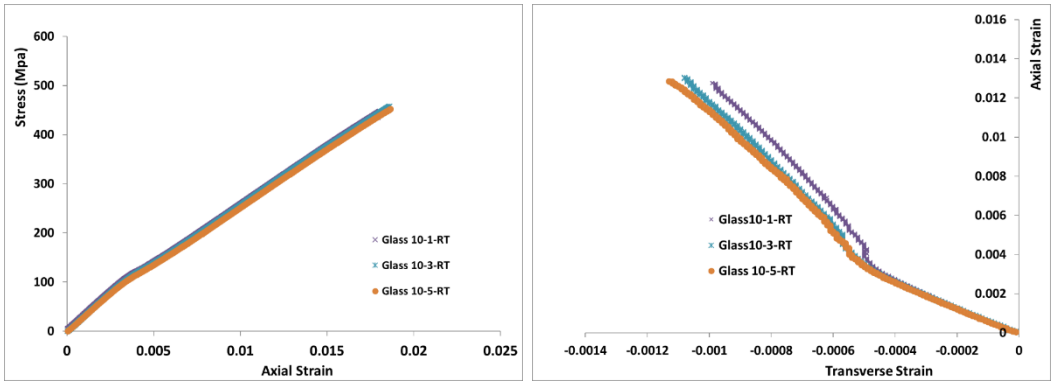

Figure 9. (a) Axial strain versus stress, (b) axial versus transverse strain for glass fiber composite (UF-3362/E-glass) specimens loaded along 0° at 25°C.

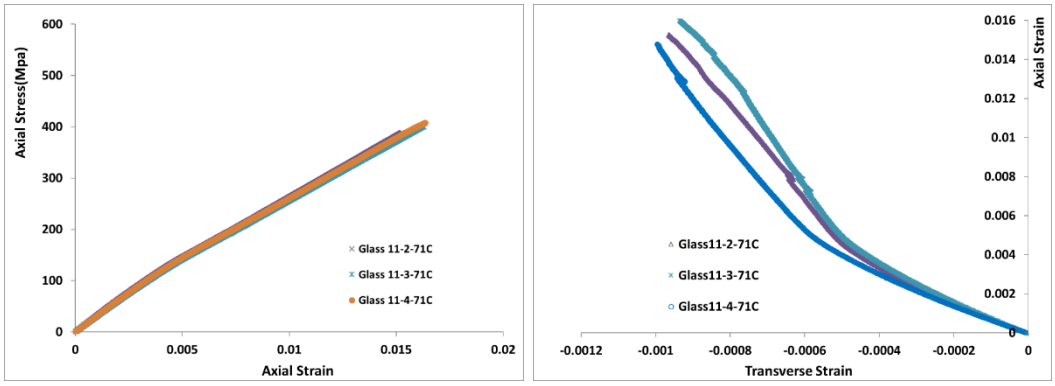

Figure 10. (a) Axial strain versus stress, (b) axial versus transverse strain for glass fiber composite (UF-3362/E-glass) specimens loaded along 0° at 71°C.

Table 8. Mechanical Properties of Glass Fiber Composites Loaded along 0° at -54°C

Sample	Ultimate Axial Strain	Ultimate Trans strain	Ultimate Stress (Mpa)	Youngs modulus(Gpa)	Poisson Ratio
C11-1	0.02160		477	36.0	0.158
C10-2	0.02002		590	38.6	
C10-4	0.02024	0.00064	510	32.8	0.148
C10-6	0.02051	0.00071	560	36.9	0.168
Average	0.02059	0.00068	534	36.1	0.16
Std dev	0.00070	0.00005	50	2.4	0.01

Table 9. Mechanical Properties of Glass Fiber Composites Loaded along 0° at 25°C

		(RT) Plate #10 - 0^0			
Sample	Ultimate Axial Strain	Ultimate Trans strain	Ultimate Stress(Mpa)	Youngs modulus(Gpa)	Poisson Ratio
C10-1	0.01800	0.00074	446	31.44	0.142
C10-3	0.01850	0.00092	458	31.60	0.149
C10-5	0.01857	0.00103	451	30.85	0.149
Average	0.01836	0.00090	452	31.30	0.1468
Std dev	0.00031	0.00015	6	0.40	0.00373

Table 10. Mechanical Properties of Glass Fiber Composites Loaded along 0° at 71°C

		(71C) Plate #11 - 0^0			
Sample	Ultimate Axial Strain	Ultimate Trans strain	Ultimate Stress(Mpa)	Youngs modulus (Gpa)	Poisson Ratio
C11-2	0.01510	0.000965	384	30.89	0.119
C11-3	0.01617	0.000951	398	29.45	0.113
C11-4	0.01628	0.001090	406	30.41	0.132
Average	0.01585	0.001002	396	30.25	0.1212
Std dev	0.00065	0.000077	11	0.73	0.0097

3.3. Summary and Comparison of Mechanical Properties

Using the above experimental method and procedure, three specimens from each of the remaining composite plates in Table 1 and 2 were tested. The ultimate stress and strain were acquired directly from the measurement while the modulus and Poisson's ratio were calculated from the stress~strain curves and the axial~transverse strain curves.

To understand the temperature effect on the mechanical properties of both carbon and glass composites, these mechanical properties were summarized in Table 11 for carbon composite and in Table 12 for glass composite from the first batch, using temperature as a variable for comparison. In order to clearly visualize the temperature effect on the mechanical parameters at the cold and hot temperatures, these values were normalized relative to the values

at room temperature. The normalized values of ultimate stress and strain, Young's modulus and Poisson's ratio are displayed in Figure 11 for carbon composite and in Figure 12 for glass composite.

From Figure 11(a), we can see that the ultimate stresses in warp (σ_{11f}) and weft directions (σ_{22f}) increased about 5% with the temperature increase from cold temperature of -54°C to room temperature and from room temperature to hot temperature of 71°C. However, the ultimate stress along 45° ($\sigma_{45^o f}$) did not show clear trend of temperature effect. Figure 11(b) shows that the values of all ultimate strains ε_{11f} ε_{22f} ε_{45f} increased with the increase of temperature. Figure 11(c) and (d) show that both young's moduli ($E_{11,}$ E_{22}) and Poisson's ratio ν_{12} ν_{21} in warp and weft directions did not show clear trend of temperature effect, however, bulk modulus G_{12} decreased with the increase of temperature and Poisson's ratio along 45° (ν_{45^o}) increased with the increase of temperature.

Figures 12(a)-(d) show the normalized values of the ultimate stresses and strains, moduli and Poisson's ratio for glass composite loaded at different directions and temperatures relative to those from room temperature. Figure 12(a) shows that the ultimate stresses in warp (σ_{11f}) and weft directions (σ_{22f}), as well as in 45° ($\sigma_{45^o f}$) all decreased with the temperature increase. Figure 12(b) shows that the values of ultimate strains ε_{11f} ε_{22f} decreased with the temperature increase while ultimate strain along 45° (ε_{45f}) increased with the temperature increase. Figure 12(c) shows that young's moduli ($E_{11,}$ E_{22}) and bulk modulus G_{12} decreased with the temperature increase. Figure 12(d) shows that Poisson's ratio (ν_{12},ν_{21}) decreased with the temperature increase, however, Poisson's ratio along 45° (ν_{45^o}) increased with the temperature increase.

Table 11. The mechanical parameters for carbon composite (UF-3362/Carbon-AS4C) specimens loaded at three different temperatures.

Temperature (°C)	Material	σ_{11f} (Mpa)	σ_{22f} (Mpa)	σ_{45of} Mpa	ε_{11f}	ε_{22}	ε_{45o}
-54	Carbon	787	861	135	0.0111	0.0121	0.0092
25	Carbon	820	897	149	0.0114	0.0135	0.0809
71	Carbon	857	926	132	0.0124	0.0134	0.1022
Temperature (°C)	**Material**	**E_{11} (Gpa)**	**E_{22} (Gpa)**	**G_{12} (Gpa)**	**ν_{12}**	**ν_{21}**	**ν_{45o}**
-54	Carbon	70.06	67.24	5.07	0.044	0.0527	0.720
25	Carbon	70.56	64.67	4.15	0.044	0.0305	0.808
71	Carbon	72.66	67.65	2.70	0.035	0.0447	0.826

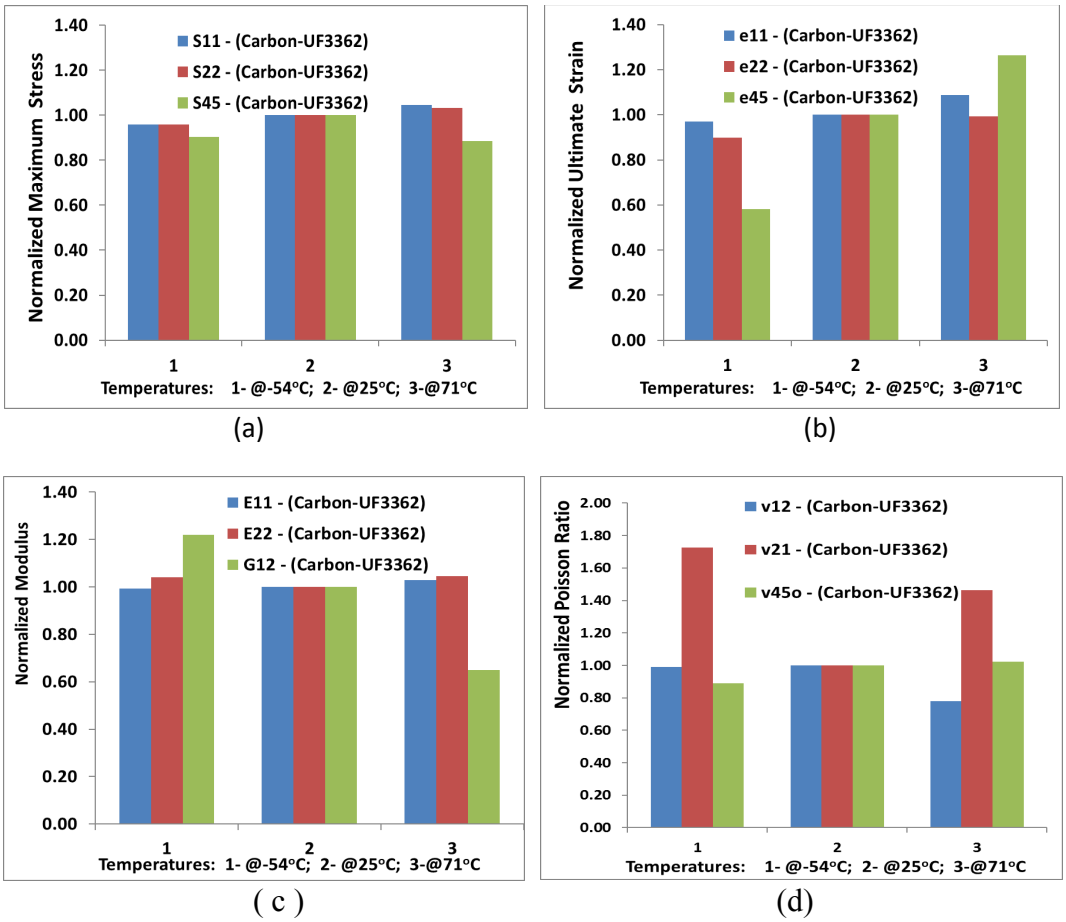

Figure 11. The normalized values of (a) ultimate stress, (b) ultimate strain, (3) Young's modulus, (d) Poisson's ratio for carbon composite showing the temperature effect on these parameters

Table 12. The mechanical parameters for glass composite (UF-3362/E-Glass) specimens loaded at three different temperatures

Temperature (°C)	Material	σ_{11f} (Mpa)	σ_{22f} (Mpa)	$\sigma_{45^\circ f}$ (Mpa)	ε_{11f}	ε_{22}	ε_{45o}
-54	Glass	534	531	203	0.0111	0.0121	0.0092
25	Glass	452	462	160	0.0114	0.0135	0.0809
71	Glass	396	430	131	0.0124	0.0134	0.1022
Temperature (°C)	**Material**	**E_{11} (Gpa)**	**E_{22} (Gpa)**	**G_{12} (Gpa)**	**ν_{12}**	**ν_{21}**	**ν_{45o}**
-54	Glass	36.06	33.26	6.05	0.158	0.1511	0.459
25	Glass	31.30	30.77	5.13	0.147	0.1336	0.550
71	Glass	30.25	27.63	3.19	0.121	0.1089	0.663

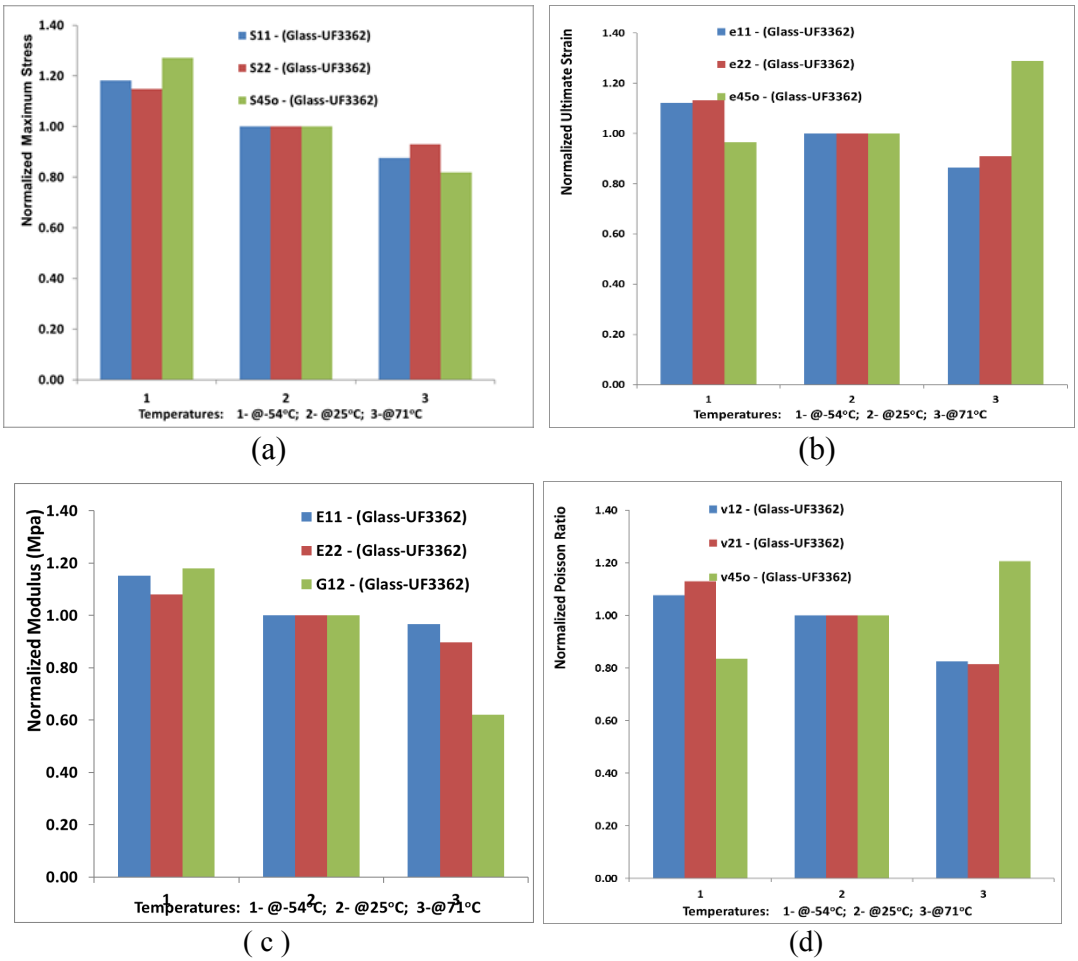

Figure 12. The normalized values of (a) ultimate stress, (b) ultimate strain, (3) Young's modulus, (d) Poisson's ratio for glass composite showing the temperature effect on these parameters

To compare the different mechanical properties along the different loading directions of 0°, 22.5°, 45°, 67.5°, 90° at three temperatures of -54°C, 25°C and 71°C, these mechanical properties were summarized in Table 13 for carbon composite and in Table 14 for glass composite using loading direction as a variable for each temperature. To clearly visualize the variation of these mechanical properties along different loading directions, the ultimate stress and strain, Young's modulus and Poisson's ratio are displayed as a function of loading angles in Figure 13 side by side for carbon composite and glass composite.

Table 13. The mechanical parameters for carbon composite (UF-3362/Carbon-AS4C) specimens loaded along different directions.

Material	Temperature	angle	Ultimate strength(Mpa)		Ultimate Strain		Poisson Ratio		Young's modulus (Gpa)	
	(^{o}C)		Average	Std dev	Average	Std dev	Average	Std dev	Average	Std dev
Carbon	-54									
		0	786.75	32.63	0.011	0.000	0.044	0.007	70.06	1.50
		22.5	237.00	11.53	0.059	0.007	0.622	0.020	13.92	2.35
		45	134.67	1.53	0.046	0.005	0.720	0.036	17.77	0.64
		67.5	237.00	2.00	0.080	0.013	0.422	0.079	14.20	2.87
		90	860.50	12.71	0.012	0.000	0.053	0.016	67.24	2.42
	25									
		0	825.00	24.15	0.011	0.000	0.045	0.006	70.82	2.21
		22.5	235.00	10.39	0.091	0.010	0.734	0.087	20.42	1.73
		45	149.00	5.20	0.081	0.007	0.808	0.047	14.86	0.29
		67.5	233.25	2.50	0.084	0.004	0.574	0.019	20.45	0.78
		90	896.50	16.11	0.013	0.000	0.031	0.010	64.67	1.83
	71									
		0	856.60	42.58	0.012	0.001	0.035	0.007	72.66	3.06
		22.5	198.33	2.89	0.097	0.003	0.712	0.069	16.50	1.75
		45	131.80	2.86	0.102	0.004	0.826	0.044	10.06	0.80
		67.5	199.67	1.00	0.087	0.001	0.598	0.061	17.93	2.18
		90	926.40	9.56	0.013	0.001	0.045	0.012	67.65	1.51

Table 14. The mechanical parameters for glass composite (UF-3362/E-Glass) specimens loaded along different directions.

Material	Temperature	angle	Ultimate strength(Mpa)		Ultimate Strain		Poisson Ratio		Young's modulus (Gpa)	
	(^{o}C)		Average	Std dev	Average	Std dev	Average	Std dev	Average	Std dev
Glass	-54									
		0	534.25	50.45	0.021	0.001	0.158	0.010	36.06	2.44
		22.5	235.00	6.24	0.060	0.006	0.299	0.035	13.92	2.35
		45	203.33	7.57	0.081	0.002	0.459	0.020	18.67	0.81
		67.5	216.67	3.06	0.061	0.017	0.251	0.079	14.20	2.87
		90	530.67	6.03	0.023	0.001	0.151	0.012	33.26	1.47
	25									
		0	451.67	6.03	0.018	0.000	0.147	0.004	31.30	0.40
		22.5	173.33	5.77	0.059	0.002	0.466	0.023	13.64	0.31
		45	160.00	7.81	0.084	0.016	0.550	0.010	29.10	0.77
		67.5	183.33	13.01	0.064	0.009	0.461	0.011	13.64	0.23
		90	462.33	12.50	0.021	0.008	0.134	0.006	30.77	0.86
	71									
		0	396.00	11.14	0.016	0.000	0.121	0.010	30.25	0.73
		22.5	178.00	4.36	0.096	0.005	0.578	0.037	10.89	0.52
		45	131.00	1.73	0.108	0.006	0.663	0.013	10.67	0.48
		67.5	181.00	6.56	0.093	0.006	0.640	0.020	12.28	2.84
		90	430.33	21.22	0.019	0.002	0.109	0.007	27.63	1.49

Figures 13(a)-(d) show the values of the ultimate stress and strain, moduli and Poisson's ratio as a function of loading directions. Figure 13(a) shows that the ultimate stress as a function of loading direction for the carbon and glass fiber composites side by side. The ultimate strength is higher along the warp and weft direction and decreases as the loading angle increases to 45°. It is close to a positive polynomial function with minimum at 45°. Figure 13(b) shows that the distribution of ultimate strain ε_{11f} ε_{22f} ε_{45f} is close to a negative polynomial function of loading angle with the maximum value at 45°. Figure 13(c) shows that the distribution of young's modulus ($E_{11,}$ E_{22}) and bulk modulus G_{12} is close to a polynomial function of the loading direction with the minimum at 45° and maximum at 0° and 90°. Figure 13(d) shows that the distribution of Poisson's ratio (ν_{12},$\nu_{21,}$ ν_{45}°) is close to a negative polynomial function of loading direction with maximum at 45°. The polynomial function can be obtained by fitting these values at these loading directions. However, it has to be pointed out that the composites loaded along 0°, 45°, 90° and those loaded along 22.5° and 67.5° were from two different batches. The fiber volume fraction for each batch had noticable difference though the exact number of volume fraction was unknown. How the volume fraction affected the mechanical properties was not characterized yet. Therefore, these mechanical properties as a function can only be viewed qualitatively, but not quantitatively.

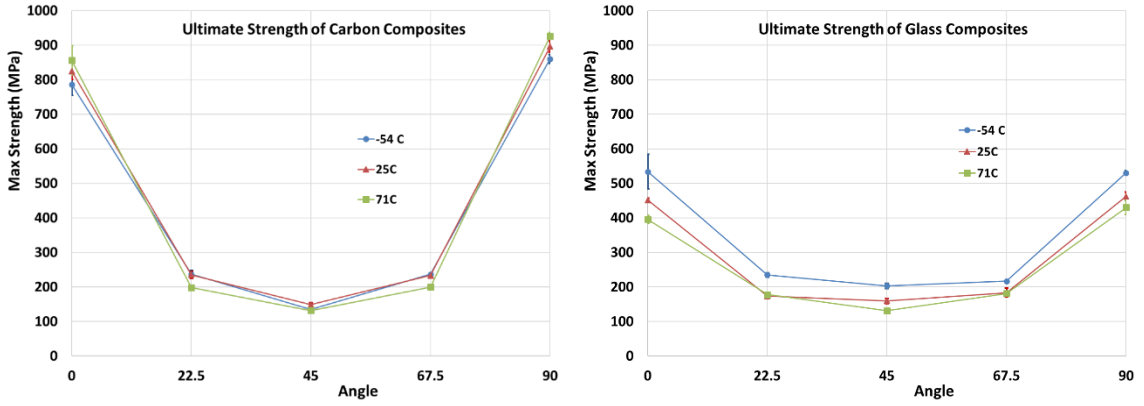

(a)

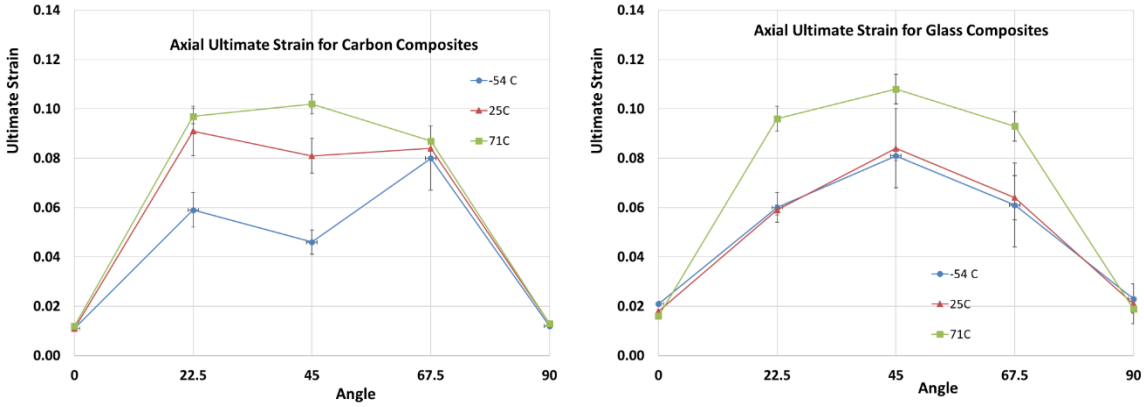

(b)

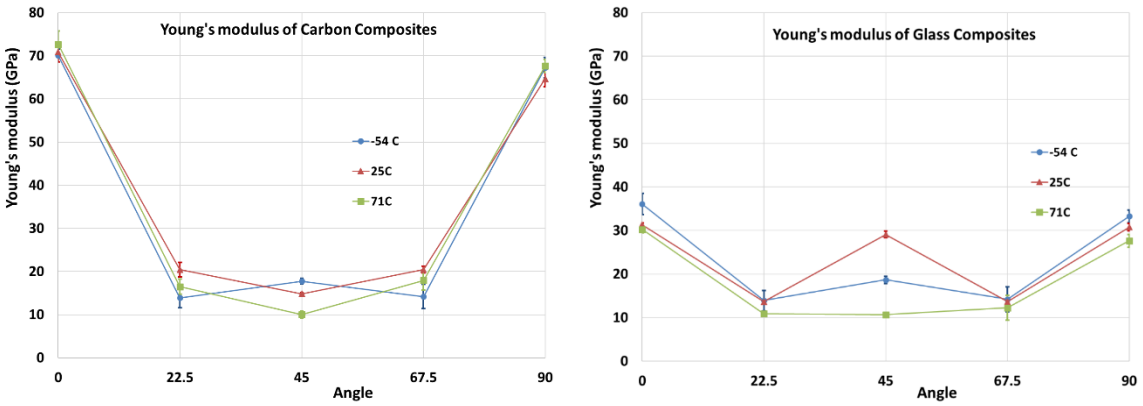

(c)

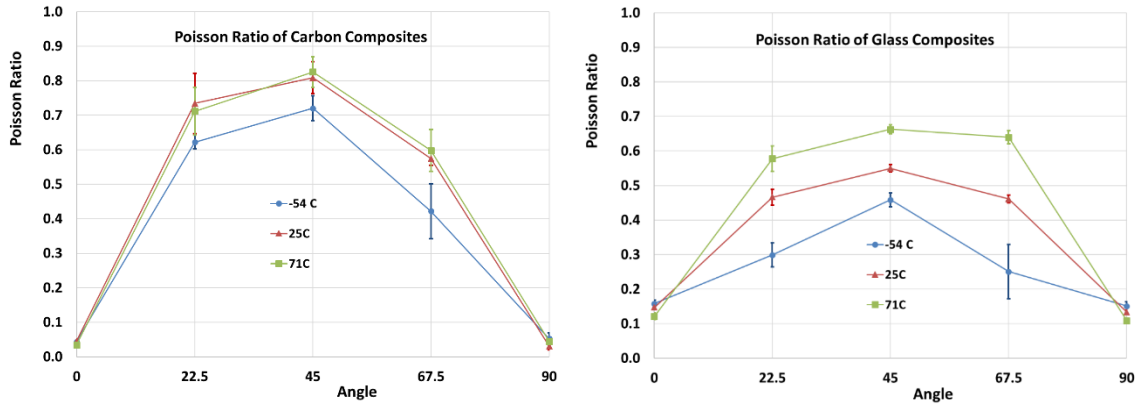

(d)

Figure 13. (a) The ultimate stress, (b) ultimate strain, (3) Young's modulus, (d) Poisson's ratio for carbon and glass composites as a function of loading directions.

5. CONCLUSIONS

In this work, we performed series of tensile tests to characterize the mechanical properties of the selected carbon composite (AS4C/UF3662) and glass composite (E-glass/UF3662) along different loading directions (0^o, 22.5^o, 45^o, 67.5^o, 90^o) at different temperatures (-54°C, 25°C, 71°C). These mechanical tests were performed with displacement rate of 2 mm/min, which was about $5x10^{(-4)}$ strain rate.

The mechanical testing data showed that the temperature had clear and consistent effects on the mechanical properties of the glass fiber composite, however the temperature effect on the carbon composite was trivial. For glass composites, the ultimate stresses in warp (σ_{11f}) and weft directions (σ_{22f}), as well as in 45^o ($\sigma_{45^o f}$) all decreased 10~20% with the temperature increase. The ultimate strains in warp and weft direction (ε_{11f} ε_{22f}) decreased 10~15% with the temperature increase. Both young's moduli (E_{11}, E_{22}), bulk modulus G_{12} and Poisson's ratio (ν_{12} ν_{21}) in warp and weft direction showed clear trend of decrease with the temperature increase. However, the ultimate strain along 45^o (ε_{45f}) and Poisson's ratio along 45^o (ν_{45^o}) increased slightly with the temperature increase. For the carbon composites, the ultimate stresses (σ_{11f} , σ_{22f}) and strains (ε_{11f} ε_{22f}) in warp and weft direction showed slight increase with the temperature increase. However, both young's moduli (E_{11}, E_{22}) and Poisson's ratios (ν_{12} ν_{21}) in warp and weft direction did not show clear trend of temperature effect. Bulk modulus G_{12} decreased slightly with the temperature increase and Poisson's ratio along 45^o (ν_{45^o}) increased slightly with the temperature increase.

The ultimate stresses and strains, moduli and Poisson's ratios at different loading directions were also characterized and compared. The ultimate stresses and Young's moduli were higher at warp and weft directions and decreased as the loading angle increased to 45^o. It was close to a polynomial function with minimum value at 45^o. The ultimate strains ε_{11f} ε_{22f} ε_{45f} and Poisson's ratios (ν_{12},ν_{21}, ν_{45^o}) were lower at warp and weft directions. They increased as the loading angle increased to 45^o. The distribution was close to a negative polynomial function of angle with maximum at 45^o.

The fiber volume fraction for first and second batch of composites need to be analyzed to study the exact fiber volume fraction effect on the mechanical properties of the composites. This will be conducted in the future work.

DISTRIBUTION LIST

1	MS9042	Scott Peterson	Org. 08343
1	MS9042	Wei-Yang Lu	Org. 08343
1	MS9042	Bonnie Antoun	Org. 08343
1	MS9042	Brian Werner	Org. 08343
1	MS9042	Helena Jin	Org. 08343
1	MS9042	Arthur Brown	Org. 08259
1	MS9042	Stacey Nelson	Org. 08259
1	MS9042	Jay Dike	Org. 08259
1	MS9106	Timothy Briggs	Org. 08222
1	MS9106	Simon Scheffel	Org. 08222
1	MS9110	Paul Yoon	Org. 08212
1	MS9154	Davina Kwon	Org. 08210
1	MS9161	Christian Mailhiot	Org. 08340
1	MS9409	Kevin Nelson	Org. 08343


Sandia National Laboratories